Analytical and Bioanalytical Chemistry (2019) 411:6319–6328
https://doi.org/10.1007/s00216-019-01814-1

RESEARCH PAPER

Unraveling altered RNA metabolism in pancreatic cancer cells by liquid-chromatography coupling to ion mobility mass spectrometry

Simon Lagies[1,2,3] · Manuel Schlimpert[1,2,3] · Lukas M. Braun[1,4] · Michel Kather[1,5,6] · Johannes Plagge[1] · Thalia Erbes[7] · Uwe A. Wittel[4] · Bernd Kammerer[1,8]

Received: 7 January 2019 / Revised: 27 February 2019 / Accepted: 27 March 2019 / Published online: 30 April 2019

Abstract

Ion mobility coupling to mass spectrometry facilitates enhanced identification certitude. Further coupling to liquid chromatography results in multi-dimensional analytical methods, especially suitable for complex matrices with structurally similar compounds. Modified nucleosides represent a large group of very similar members linked to aberrant proliferation. Besides basal production under physiological conditions, they are increasingly excreted by transformed cells and subsequently discussed as putative biomarkers for various cancer types. Here, we report a method for modified nucleosides covering 37 species. We determined collisional cross-sections with high reproducibility from pure analytical standards. For sample purification, we applied an optimized phenylboronic acid solid-phase extraction on media obtained from four different pancreatic cancer cell lines. Our analysis could discriminate different subtypes of pancreatic cancer cell lines. Importantly, they could clearly be separated from a pancreatic control cell line as well as blank medium. m1A, m27G, and Asm were the most important features discriminating cancer cell lines derived from well-differentiated and poorly differentiated cancers. Eventually, we suggest the analytical method reported here for future tumor-marker identification studies.

Keywords Modified nucleosides · Ion mobility mass spectrometry · TWIMS · Pancreatic cancer · Biomarker

Published in the topical collection *Close-Up of Current Developments in Ion Mobility Spectrometry* with guest editor Gérard Hopfgartner.

Simon Lagies and Manuel Schlimpert contributed equally to this work.

Electronic supplementary material The online version of this article (https://doi.org/10.1007/s00216-019-01814-1) contains supplementary material, which is available to authorized users.

✉ Bernd Kammerer
Bernd.Kammerer@zbsa.uni-freiburg.de

[1] Center for Biological Systems Analysis ZBSA, Albert-Ludwigs-University Freiburg, Habsburgerstr. 49, 79104 Freiburg, Germany

[2] Institute of Biology II, Albert-Ludwigs-University Freiburg, Schänzlestr. 1, 79104 Freiburg, Germany

[3] Spemann Graduate School of Biology and Medicine, Albert-Ludwigs-University Freiburg, Albertstr. 19A, 79104 Freiburg, Germany

[4] Department of General- and Visceral Surgery, University of Freiburg Medical Center, Hugstetter Str. 55, 79106 Freiburg, Germany

[5] Faculty of Chemistry and Pharmacy, Albert-Ludwigs-University Freiburg, Hebelstr. 27, 79104 Freiburg, Germany

[6] Hermann Staudinger Graduate School, University of Freiburg, Hebelstr. 27, 79104 Freiburg, Germany

[7] Department of Gynecology and Obstetrics, Faculty of Medicine and Medical Center, University of Freiburg, Hugstetter Str. 55, 79106 Freiburg, Germany

[8] BIOSS Centre for Biological Signalling Studies, University of Freiburg, Schänzlestr. 16, 79104 Freiburg, Germany

Introduction

Pancreatic carcinoma has a high mortality rate with currently more than 250,000 deaths per year and will become the second most cause of cancer-related deaths by 2030 [1, 2]. The 5-year survival rate of patients suffering from pancreatic cancer is below 5% and did not change during the last decades [3, 4]. One of the major challenges is the detection of pancreatic ductal adenocarcinoma (PDAC) at an early and curable disease stage. On the one hand, patients only rarely exhibit cardinal symptoms and, on the other hand, tumor cells do not show specific and sensitive biomarkers [5]. Pancreatic cancer is usually detected at late advanced stages when only palliative therapies are available [6]. Approximately 20% of all pancreatic cancer patients undergo curative resection, whereas more than 60% of these patients experience local or metastatic disease recurrence [7–9]. Since the carbohydrate antigen 19-9 (CA19-9) is currently the only available clinical tumor marker for PDAC, there is an urgent need of biomarkers to reliably detect pancreatic cancer and to improve patients' prognosis [10]. Due to the lack of reliable biomarkers, research is ongoing to identify other molecules in the blood of PDAC patients to specifically detect pancreatic cancer at an early stage. The attempts are summarized as liquid biopsy and include the detection of mutated cell-free DNA [11], small non-coding RNAs [12], tumor-specific antibodies [13], and tumor-specific proteins [14] as well as exosomes [15] and metabolites [16] secreted by tumor cells for the early detection of PDAC. Especially the detection of metabolites in conjunction with CA19-9 has shown promising results in screening a high-risk collective of patients with pancreatic cancer [17]. Metabolites that were previously identified as potential markers for pancreatic cancer include lipids and fatty acids [18]. Moreover, amino acids like alanine, isoleucine, leucine, lysine, and methionine were found to discriminate between pancreatic carcinoma and healthy controls [19, 20]. In general, RNA turnover is elevated in tumor tissue compared to normal tissue [21] and additionally, RNA is extensively regulated by modifications [22]. However, modified nucleosides are not subjected to the RNA salvage pathway and consequently excreted into urine [23]. Therefore, modified nucleosides are discussed as tumor markers for various malignancies such as breast cancer, urothelial bladder cancer, or colorectal cancer [24–26].

The emerging field of metabolomics encounters, more than the other omics sciences, difficulties in the coverage of the whole metabolome due to its high chemical diversity of compound classes such as small amino acids, sugars, tricarboxylic acids, and nucleotides to lipids. Therefore, the analysis of the whole metabolome with one method is impossible so far. As a consequence, many different methods are applied in the field of metabolomics. Two main techniques are commonly applied as detector systems, i.e., nuclear magnetic resonance (NMR) and mass spectrometry (MS). NMR offers some advantages for structural elucidation and the possibility of in vivo measurements is however also limited by the required amount of sample. Mass spectrometry enables both high sensitivity and structural elucidation. Due to the vast diversity of metabolites, scientists use different techniques like gas chromatography coupled to an electron impact mass spectrometer or liquid chromatography coupled to a triple quadrupole MS or a high-resolution MS (ToF, Orbitrap). For the analysis of modified nucleosides, reversed-phase liquid chromatography coupled to various types of mass spectrometers has been commonly reported in the past [27, 28]. In the last decade, a new technique became available in the metabolomics toolkit: ion mobility [29]. Ion mobility can resolve different analytes based on their charge, size, and shape [30]. Ions are accelerated by electric force against a gas stream and thus separated by their respective drift time. Currently, there are different technologies used for coupling of IMS to MS such as traveling wave IMS (TWIMS) [31, 32], drift-tube IMS (DTIMS) [33], or trapped IMS (TIMS) [34]. Several studies aimed at resolving complex matrices by direct infusion experiments in an IMS-ToF-MS, already including the analysis of nucleic acids. Kanu et al. achieved separation of DNA nucleosides from their mono-, di-, and triphosphates by direct infusion [35]. They suggested this fast method (less than 1 min) for future DNA sequencing techniques. Quinn and colleagues were challenged by the differentiation of isobaric nucleotides and published a method for discriminating adenosine monophosphate from deoxyguanosine monophosphate as well as uridine monophosphate from pseudouridine monophosphate also by direct infusion experiments [36]. Rose et al. established an elegant direct infusion experiment for modified nucleosides on the transcriptome level, covering the broadest range of nucleosides so far [37]. All these studies used direct infusion experiments, as they intended to analyze nucleic acids derived from macromolecules, which had been purified beforehand resulting in a relatively pure matrix. It will however become necessary to apply chromatographic separation when analyzing nucleosides within a complex metabolite mixture. Otherwise, ion suppression can significantly impair the detection of the target molecules. Additionally, all of these studies aimed at separating the nucleosides/nucleotides from each other and did not report system- and method-independent collisional cross-sections (CCS) as a unique chemical property of the analytes.

Our study focused on modified nucleosides that could potentially serve as biomarkers for early-stage pancreatic cancer. Therefore, we developed an LC-IMS-MS method for the detection of free nucleosides and their modifications considering their CCS values for additional identification certitude. In a first approach, we screened cell culture supernatant from four different pancreatic cancer cell lines and one normal pancreas cell line for modified

Table 1 Origin of the cell lines used in this study

Cell line	Capan2	HPAFII	MiaPaCa2	Panc1
Age	56	44	65	56
Sex	Male	Male	Male	Female
Derivation	Primary tumor	Ascites	Primary tumor	Primary tumor
Metastasis	No	Yes	ND	Yes
Differentiation	Well	Well	Poor	Poor
EMT	Epithelial	Epithelial	Mesenchymal	Mesenchymal
KRAS	12 Val	12 Asp	12 Cys	12 Asp
TP53	WT/Intron 4 Δ200-bp splice site	151 Ser	248 Trp	273 His/ 273 Cys
CDKN2A/p16	WT/6-7 bp insertion	HD (Δ20–25/Δ26–27/Δ29–34)	HD	HD
SMAD4/DPC4	WT	WT	WT	WT
References	[38–41]	[38, 39, 41–43]	[39, 41, 43–45]	[38, 39, 41, 43, 45, 46]

nucleosides. We present a panel of modified nucleosides secreted by pancreatic cancer cell lines but not the control cell line. Further studies are necessary to evaluate and confirm these results in patient serum samples.

Materials and methods

Cell culture and culture conditions

The established pancreatic cancer cell lines Capan2, HPAFII, MiaPaCa2, and Panc1 were originally purchased from the American Type Culture Collection (ATCC, see Table 1). The control pancreatic cell line KHM1106 was established and provided from one surgical specimen after pancreas resection. Informed consent was obtained for KHM1106 cell line usage and approved by the local Ethics Committee Freiburg (126/17 and 371/14) and registered at the German Clinical Trials Register (DRKS-ID DRKS00007561). All cells were grown in DMEM high glucose medium containing GlutaMAX™ and pyruvate (Life Technologies, Darmstadt, Germany), supplemented with 10% Fetal Bovine Serum (Life Technologies, Darmstadt, Germany) as well as 100 U/mL penicillin and 100 µg/mL streptomycin (Life Technologies, Darmstadt, Germany). The cells were incubated at 37 °C and 5% CO_2 in a humidified atmosphere.

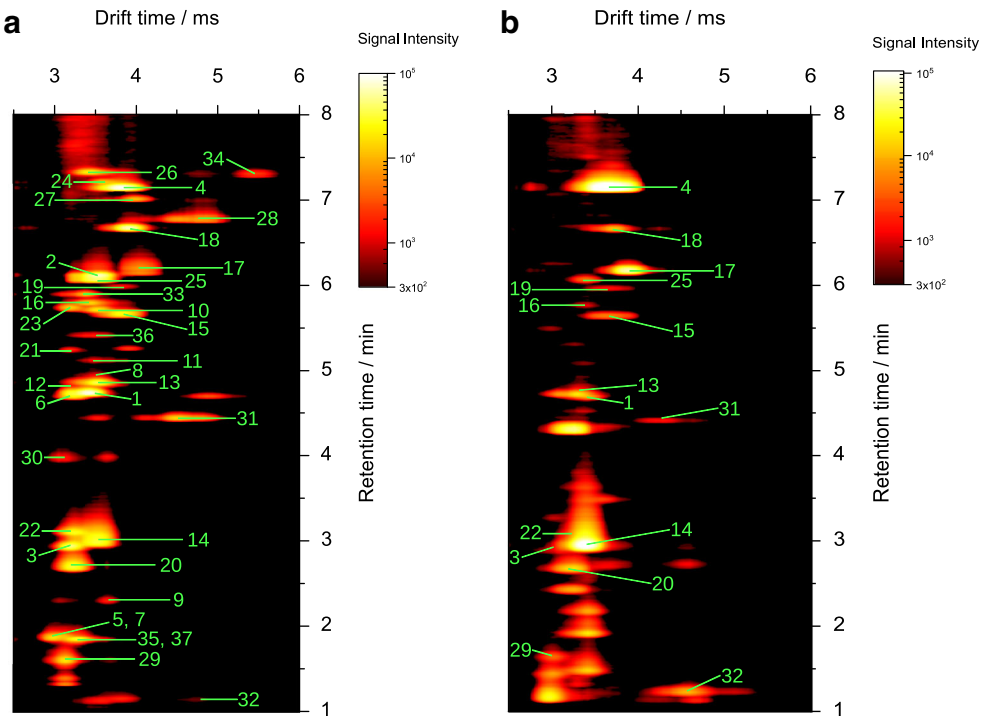

Fig. 1 Overlaid EICs of the analyzed nucleosides. Numbering according to Table 2. **a** Analysis of nucleoside standard mix. **b** Analysis of nucleosides in MiPaCa2 medium

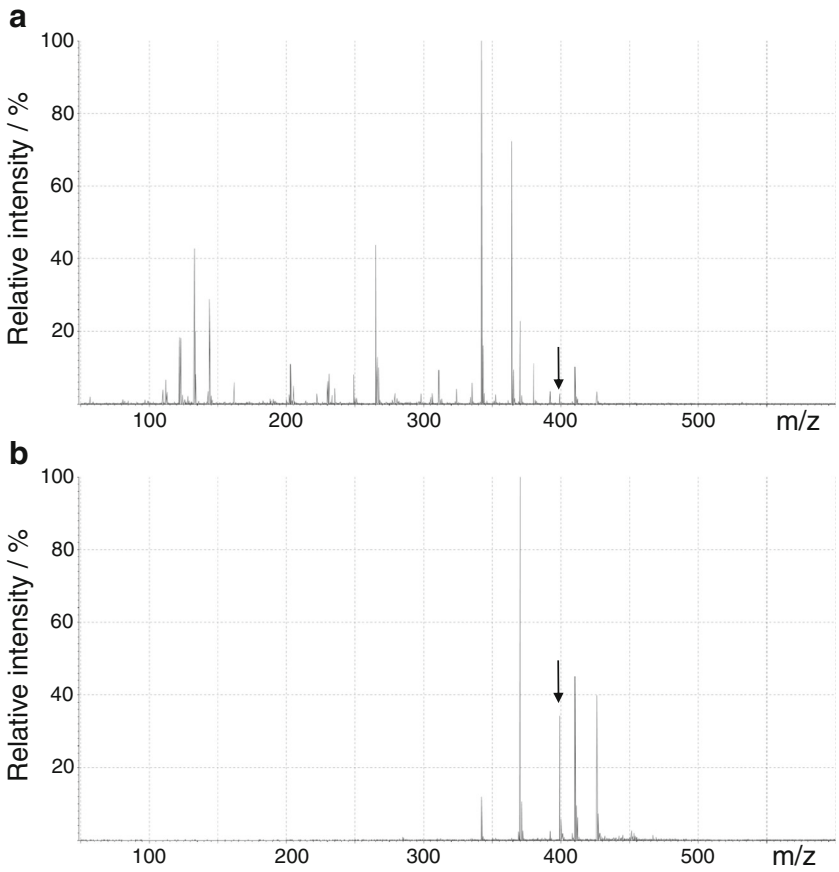

Fig. 2 Addition of ion mobility lead to increased spectral cleanliness as shown for SAM (arrow): **a** shows the whole spectrum at the retention time of SAM, while **b** shows the spectrum only at the corresponding drift time

Cells were seeded in 75-cm^2 plastic flasks (Sarstedt, Nümbrecht, Germany) and passaged at least once a week at around 70% confluency. For cell seeding, cells were washed with × 1 PBS (Life Technologies, Darmstadt, Germany) and incubated with 0.05% Trypsin/EDTA (Life Technologies, Darmstadt, Germany) at 37 °C and 5% CO_2. Cells were counted using a TC20™ Automated Cell Counter (BioRad, München, Germany). 1×10^6 cells were seeded in 12 mL of culture medium and incubated as described above until reaching 90% confluency. The culture medium was replaced twice a week. For nucleoside analysis, the culture medium was harvested, centrifuged at 350*g* for 5 min and immediately frozen at − 80 °C.

Nucleoside extraction/extraction of *cis*-diols

Nucleosides were extracted using Bond Elut Phenylboronic Acid (PBA) solid-phase extraction (SPE) columns (500 mg, 6 mL) (Agilent, Waldbronn, Germany). Cell culture medium samples were thawed at room temperature, spiked with isoguanosine as internal standard to a concentration of 0.5 μg/mL, and alkalized to pH 9.9 with ammonia solution. SPE was performed under vacuum. The columns were equilibrated with 2 × 5 mL acetonitrile/water (7:3, *v/v*) acidified with 1% formic acid, followed by 2 × 5 mL methanol/water (1:1, *v/v*), 2 × 5 mL ammonium acetate solution (250 mM, pH 9.9), 2 × 5 mL methanol/water (1:1, *v/v*), 2 × 5 mL acetonitrile/water (7:3, *v/v*) acidified with 1% formic acid, 2 × 5 mL methanol/water (1:1, *v/v*), and 2 × 5 mL ammonium acetate solution (250 mM, pH 9.9). Afterwards, the cell culture medium sample was applied to the column. Washing steps were performed with 2 × 5 mL ammonium acetate solution (250 mM, pH 9.9) and 4 × 5 mL methanol/water (1:1, *v/v*). Nucleosides were eluted with 6 mL methanol/water (1:1, *v/v*) acidified with 1% formic acid. One milliliter of the eluate was evaporated and the pellet was resuspended in 100 μL water for analysis.

Chromatography, mass spectrometry, and ion mobility

A Waters UPLC i-Class coupled to a Synapt G2Si was used. The sample manager was kept at 8 °C. A Waters BEH-C18 column (1.8-μm particle size, 2.1 × 100 mm) was kept at 40 °C. The chromatography program was 99.9% A (A: water with 0.1% formic acid, B: methanol with 0.1% formic acid) hold for 2 min, to 85% A within 3 min, to 50% A within 1.5 min, and to 2% A within 1.5 min, hold for 4 min. Re-equilibration was achieved within 3 min. The flow rate was set to 200 μL/min.

Table 2 Summary of the analyzed nucleosides with the corresponding numbering and abbreviation used throughout this manuscript. The expected mass to charge ratios were calculated by the molecular mass calculator from the RNA Modification Database [50]. Retention time (RT), arrival time distribution (ATD) apices, and CCS values are shown with the corresponding 95% confidence intervals

No.	Abbreviation	Compound	Formula	$[M+H]^+$ (exp) z/m	RT ± 95% confidence interval/min	ATD ± 95% confidence interval/ms	CCS ± 95% confidence interval/Å^2
1	A	Adenosine	$C_{10}H_{13}N_5O_4$	268.1040	4.74 ± 0.01	3.41 ± 0.00	157.1 ± 0.5
2	ac4C	N^4-Acetylcytidine	$C_{11}H_{15}N_3O_6$	286.1034	6.14 ± 0.00	3.53 ± 0.00	160.1 ± 0.4
3	AICAR	5-Aminoimidazol-4-carboxamid-1-β-D-ribofuranoside	$C_9H_{14}N_4O_5$	259.1037	2.94 ± 0.01	3.18 ± 0.00	152.2 ± 0.4
4	Asm	5-Deoxy-5-methylthioadenosine	$C_{11}H_{15}N_5O_3S$	298.0968	7.16 ± 0.01	3.85 ± 0.00	166.1 ± 0.1
5	C	Cytidine	$C_9H_{13}N_3O_5$	244.0928	1.93 ± 0.01	2.98 ± 0.00	148.6 ± 0.1
6	Cm	2′-O-Methylcytidine	$C_{10}H_{15}N_3O_5$	258.1084	4.67 ± 0.05	3.14 ± 0.00	152.2 ± 0.2
7	D	5,6-Dihydrouridine	$C_9H_{14}N_2O_6$	247.0925	1.86 ± 0.15	2.98 ± 0.00	147.7 ± 0.2
8	G	Guanosine	$C_{10}H_{13}N_5O_5$	284.0989	4.86 ± 0.01	3.53 ± 0.00	159.9 ± 0.3
9	Ho5U	5-Hydroxyuridine	$C_9H_{12}N_2O_7$	261.0717	2.34 ± 0.00	3.10 ± 0.00	149.8 ± 0.1
10	Ho8d2G	8-Hydroxy-2′-deoxyguanosine	$C_{10}H_{13}N_5O_5$	284.0989	5.74 ± 0.01	3.49 ± 0.00	158.6 ± 0.3
11	Ho8G	8-Hydroxyguanosine	$C_{10}H_{13}N_5O_6$	300.0939	5.14 ± 0.01	3.53 ± 0.00	159.9 ± 0.4
12	I	Inosine	$C_{10}H_{12}N_4O_5$	269.0880	4.87 ± 0.02	3.30 ± 0.00	155.0 ± 0.3
13	IsoG	Isoguanosine	$C_{10}H_{13}N_5O_5$	284.0989	4.68 ± 0.01	3.45 ± 0.00	158.0 ± 0.3
14	m1A	N^1-Methyladenosine	$C_{11}H_{15}N_5O_4$	282.1197	2.97 ± 0.03	3.57 ± 0.00	160.0 ± 0.2
15	m1G	N^1-Methylguanosine	$C_{11}H_{15}N_5O_5$	298.1146	5.68 ± 0.00	3.69 ± 0.00	163.1 ± 0.2
16	m1I	1-Methylinosine	$C_{11}H_{14}N_4O_5$	283.1037	5.81 ± 0.00	3.45 ± 0.00	158.4 ± 0.2
17	m227G	N^2,N^2,N^7-Trimethylguanosine	$C_{13}H_{19}N_5O_5$	326.1459	6.18 ± 0.02	4.08 ± 0.00	170.6 ± 0.3
18	m27G	N^2,N^7-Dimethylguanosine	$C_{12}H_{17}N_5O_5$	312.1302	6.69 ± 0.00	3.91 ± 0.03	167.5 ± 0.2
19	m2G	N^2-Methylguanosine	$C_{11}H_{15}N_5O_5$	298.1146	5.99 ± 0.00	3.73 ± 0.00	163.9 ± 0.2
20	m3C	3-Methylcytidine	$C_{10}H_{15}N_3O_5$	258.1084	2.70 ± 0.03	3.26 ± 0.00	153.5 ± 0.2
21	m3 U	3-Methyluridine	$C_{10}H_{14}N_2O_6$	259.0925	5.25 ± 0.00	3.18 ± 0.00	151.3 ± 0.2
22	m5C	5-Methylcytidine	$C_{10}H_{15}N_3O_5$	258.1084	3.08 ± 0.03	3.18 ± 0.00	152.7 ± 0.1
23	m5 U	5-Methyluridine	$C_{10}H_{14}N_2O_6$	259.0925	5.75 ± 0.01	3.14 ± 0.00	151.6 ± 0.1
24	m62A	N^6,N^6-Dimethyladenosine	$C_{12}H_{17}N_5O_4$	296.1353	7.23 ± 0.00	3.59 ± 0.04	160.9 ± 0.3
25	m6A	N^6-Methyladenosine	$C_{11}H_{15}N_5O_4$	282.1197	6.09 ± 0.00	3.40 ± 0.03	158.3 ± 0.2
26	m6I	N^6-Methylinosine	$C_{11}H_{14}N_4O_5$	283.1037	7.35 ± 0.00	3.41 ± 0.00	156.6 ± 0.1
27	mcm5s2U	5-Methoxy-carbonylmethyl-2-thiouridine	$C_{12}H_{16}N_2O_7S$	333.0751	7.03 ± 0.00	3.96 ± 0.00	169.0 ± 0.2
28	N6SA	N^6-Succinyloadenosine	$C_{14}H_{17}N_5O_8$	384.1150	6.79 ± 0.00	4.83 ± 0.00	185.2 ± 0.1
29	NAR	1-Ribosyl-imidazolenicotinamide	$[C_{11}H_{15}N_2O_5]^+$	255.0975 (−e)	1.64 ± 0.01	3.18 ± 0.00	152.1 ± 0.2
30	s2C	2-Thiocytidine	$C_9H_{13}N_3O_4S$	260.0699	3.92 ± 0.03	3.14 ± 0.00	150.9 ± 0.2
31	SAH	S-Adenosyl-homocysteine	$C_{14}H_{20}N_6O_5S$	385.1289	4.40 ± 0.01	4.53 ± 0.04	179.8 ± 0.2
32	SAM	S-Adenosyl-methionine	$[C_{15}H_{23}N_6O_5S]^+$	399.1445 (−e)	1.22 ± 0.02	4.75 ± 0.00	185.0 ± 0.2
33	T	Thymidine	$C_{10}H_{14}N_2O_5$	265.0801 (+Na)	5.91 ± 0.00	3.41 ± 0.00 (+Na)	158.9 ± 0.3 (Na)
34	t6A	N^6-Threonyl-carbamoyl-adenosine	$C_{15}H_{20}N_6O_8$	413.1415	7.31 ± 0.00	5.46 ± 0.00	196.9 ± 0.3
35	U	Uridine	$C_9H_{12}N_2O_6$	245.0768	1.90 ± 0.01	2.90 ± 0.00	146.6 ± 0.1
36	X	Xanthosine	$C_{10}H_{12}N_4O_6$	285.0830	5.43 ± 0.01	3.47 ± 0.04	158.1 ± 0.4
37	Y	Pseudouridine	$C_9H_{12}N_2O_6$	245.0768	1.90 ± 0.01	2.98 ± 0.00	147.1 ± 0.2

The Waters Synapt G2Si, which uses traveling wave ion mobility spectrometry (TWIMS), was optimized regarding IMS resolution for the desired mass range (50–600 m/z) and reduction of in-source fragmentation as well as fragmentation within the IMS cell. This was necessary due to the lower resolving power of TWIMS (up to 45) when compared to drift-tube IMS (DTIMS, resolving power 58-77) or trapped IMS (TIMS, resolving power 154-183). A review comparing these different metrics and difficulties when comparing the different IMS platforms was recently published [47]. The

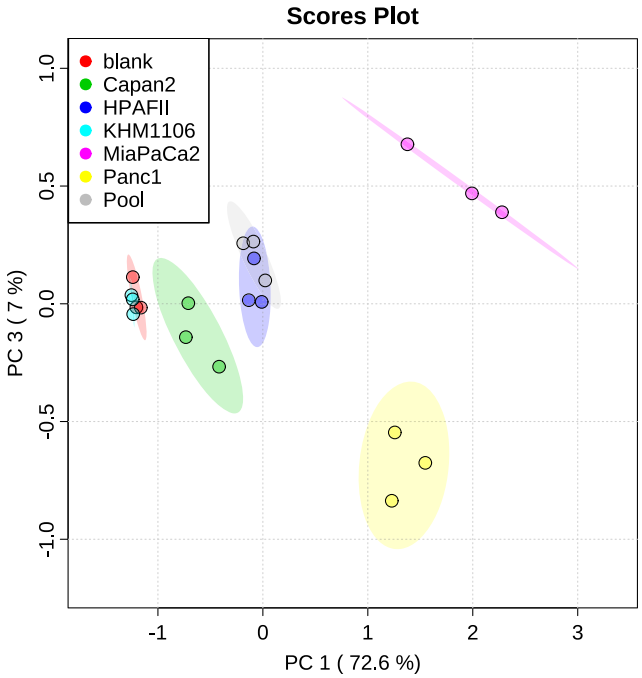

Fig. 3 Principal component analysis of modified nucleosides obtained by SPE from blank medium and media from a pancreatic control cell line (KHM1106) and four cancer cell lines. No global difference between blank and control cell line could be detected, whereas the four cancer cell lines clearly separated from them. PC2 is not shown in this figure as it reflected the biological and technical variance with 9.4%. $n = 3$

optimized mass spectrometry and IMS settings are displayed in Table S1 in the Electronic Supplementary Material (ESM). The mass calibration was executed with 0.5 mM sodium formate in isopropanol/water (8:2, *v*/*v*) and the CCS calibration with Waters Major Mix.

For data analysis, Waters Unifi (Version 1.9.2.045) was used with default settings for HDMSe analysis with the exceptions listed in ESM Table S2. CCS values were calculated with Unifi. This calculation is based on a power function for dynamic electric fields derived from the Mason-Schamp equation as described in detail by Smith and coworkers [48]. The factor and exponent in that equation was determined by CCS calibration with Waters Major Mix. For each analyte, reduced mass, charge, and drift time were determined. Intensities were normalized to isoguanosine. ANOVA was executed followed by FDR correction. Resulting *q*-values below 0.05 were considered significant. Significant pairs were detected by Tukey's post hoc analysis. For principal component analysis, heat map generation, and VIP score calculation, the intensities were further range-scaled. This was executed by MetaboAnalyst 4.0 [49]. Extracted ion chromatograms were visualized by Origin and Inkscape.

Data availability

The raw data of this publication will be publically available from the MetaboLights repository under the study identifier MTBLS812 (https://www.ebi.ac.uk/metabolights/MTBLS812). The results of statistical analysis are displayed in ESM Table S3.

Results

The combination of reversed-phase ultra-performance liquid chromatography with ion mobility leads to excellent separation of nucleosides as shown in Fig. 1a for a standard mixture and for a biological matrix (Fig. 1b). Corollary, addition of ion mobility leads to an increased spectral cleanliness as exemplarily shown for S-adenosylmethionine (Fig. 2).

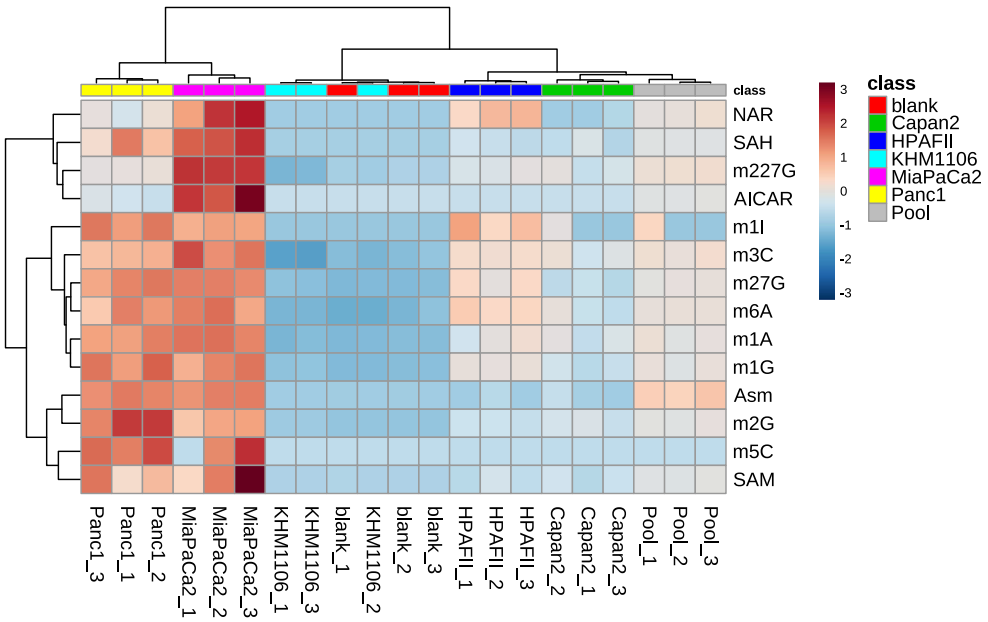

Fig. 4 Heat map of significantly (ANOVA, FDR-corrected *q*-value < 0.05) changed nucleosides in cell culture media from four pancreatic cancer cell lines, control cell, and blank media. Intensities were normalized to internal standard (isoguanosine) and range-scaled

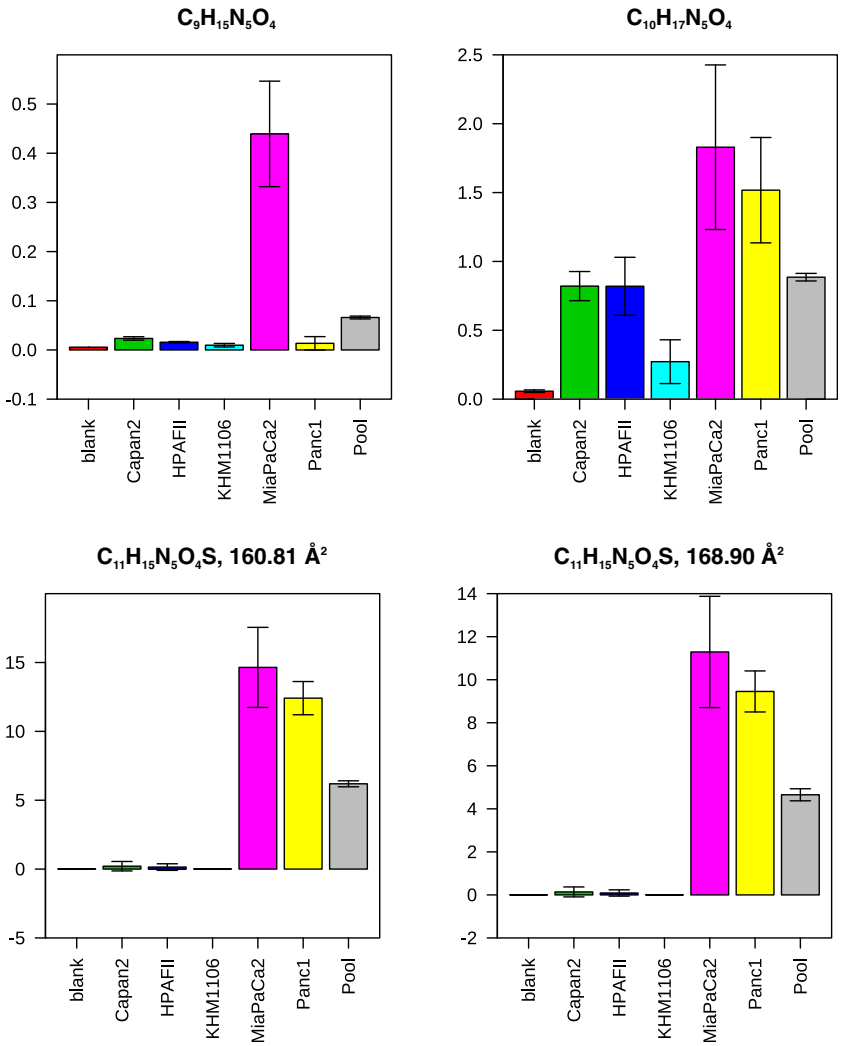

Fig. 5 Summary of detection results for the putative modified nucleosides. Intensities were normalized to isoguanosine. $C_9H_{15}N_5O_4$ was higher in MiaPaCa2 than in all other samples, whereas the other three species were in general higher in MiaPaCa2 and Panc1 compared to all the other groups. $C_{10}H_{17}N_5O_4$ was also elevated in Capan2 and HPAFII compared to KHM1106 and blank medium. $n = 3$

Chromatographic reproducibility was assessed by measuring retention time of pure analytical standards thrice and revealed an average relative standard deviation (RSD) of 0.27%. Arrival time distribution (ATD) apices and the corresponding CCS values, which were determined after calibration, also showed an excellent repeatability with an average RSD of 0.08%. All individual retention times, ATD apices, and CCS values with their corresponding deviations are shown in Table 2. In addition, ATDs for some isomers are shown in ESM Fig. S1.

To test our analysis for suitability of biological matrices, we analyzed cell culture media from four different pancreatic cancer cell lines (see Table 1) with corresponding controls, i.e., blank medium and a pancreatic control cell line. For this matrix, we performed a solid-phase extraction with phenylboronic acid as stationary phase. Phenylboronic acid reversibly forms covalent complexes with *cis*-diols present in ribose in a pH-dependent manner. Example ionograms for comparison of the standard mixture and a biological matrix are shown in ESM Fig. S2. Principal component analysis revealed global differences in the excreted modified nucleosides between controls and cancer cells (Fig. 3). Specifically, different subtypes could be discriminated, corresponding to different characteristics of these cell lines such as differentiation state. Principal component (PC) 1 accounted for 72.6% of the differences and leads to discrimination of three groups, i.e., controls, well differentiated, and poorly differentiated (Fig. 3). PC 2 describing 9.4% of total differences revealed the biological and technical variance (data not shown). PC 3 with 7% of observed alterations yielded a separation of Panc1 from HPAFII and MiaPaCa2 (Fig. 3). Capan2 and HPAFII were further discriminated by PC 5 with 3.7% of observed differences (data not shown).

Figure 4 shows the heat map of significantly altered modified nucleosides between all sample groups according to ANOVA ($q < 0.05$, specific results are shown in ESM Table S3). The cluster analysis after Euclidian and Ward is also included in Fig. 4 and confirms the results of the PCA: MiaPaCa2 and Panc1 were the most different pancreatic cell lines compared to the control cell

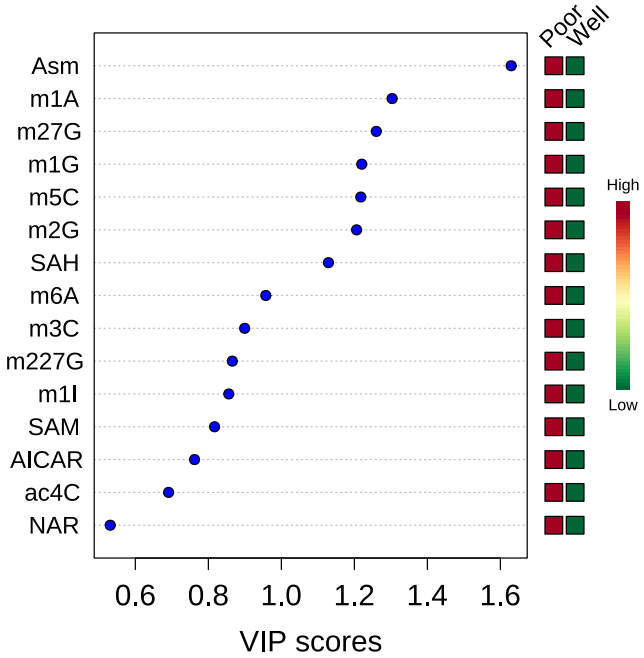

Fig. 6 PLSDA-VIP analysis between well (Capan2, HPAFII) and poorly (MiaPaCa2, Panc1) differentiated cancer cell conditioned media revealed that Asm, m1A, and m27G were the most important features

line KHM1106, followed by Capan2 and HPAFII. NAR, m227G, and AICAR lead to a discrimination of MiaPaCa2 from Panc1. NAR was also elevated in HAPAFII.

In media conditioned by pancreatic cancer cell lines, we further identified four putative nucleosides for that no analytical standards were available (ESM Table S4). The compound with 314.0916 m/z yielded two different peaks after ion-mobility separation. The fragmentation of both compounds revealed adenosine as base and no ribose loss (− 132 u). The predominant neutral loss observed in this species corresponds to a modified ribose (ribose + CH_2S, − 178 u). With all this information, we speculate that one of these peaks is 5′-deoxy-5′-methylthioadenosine-sulfoxide, which has already been discussed in the context of breast cancer [51]. The other peak might be an isomer of the first one, for example 5′-methylthioadenosine (not to be confused with 5′-deoxy-5′-methylthioadenosine).

These four putative modified nucleosides correlated with the abundance of modified nucleosides for that analytical standards were available, i.e., high abundance in MiaPaCa2 and Panc1, medium abundance in Capan2 and HPAFII, and lowest abundance in blank medium and KHM1106 (Fig. 5).

Next, we performed a partial least-square discriminant very important feature analysis with MiaPaCa2 and Panc1 as undifferentiated cell lines and HPAFII and Capan2 as differentiated ones. The differentiation state correlates with the malignancy of cancers. Asm, m1A, and m27G were the most important features for differentiation state (Fig. 6) and might therefore serve especially valuable as biomarker for this highly aggressive and mortal malignancy.

Discussion

In this study, we successfully established a method for analysis of modified nucleosides from cell culture media by LC-IMS-ToF. The injection-to-injection time of 14 min was a two- to ninefold decrease in analysis time when compared to methods with different instrumentation but the same scope [51–53]. To our knowledge, this was the first time that system-independent CCS values were reported for a broad range of modified nucleosides. Only some CCS values for unmodified nucleosides had been reported before [54]. We observed good reproducibility of chromatography and ion mobility. We decided to use an optimized protocol for phenylboronic acid SPE, while some authors prefer a reversed-phase SPE in order not to lose deoxynucleosides [52]. However, charged nucleosides are easily lost during this procedure and, in addition, the RNA pool has a much higher turnover rate than DNA and is therefore in our opinion more suitable for sensitive detection of malignancies such as pancreatic cancer. We suggest this method for future biomarker discovery studies for pancreatic cancer and other malignancies as we could successfully discriminate different subtypes of pancreatic cancer cell lines from controls as documented by unsupervised discriminant analysis. Heat map analysis and supervised VIP score generation revealed the specific modifications contributing to that discrimination. This was the first analysis of modified nucleosides in relation to pancreatic cancer.

Acknowledgements This work was supported by Project B01 of the collaborative research initiative (SFB 1140 - KIDGEM) to M.S. and B.K. by the German Research Foundation (DFG).

Author contribution Simon Lagies, Manuel Schlimpert, Lukas M. Braun, Thalia Erbes, Uwe A. Wittel, and Bernd Kammerer designed the study. Simon Lagies, Manuel Schlimpert, Lukas M. Braun, and Michel Kather performed the experiments and data analysis. Johannes Plagge aided in data processing and image creation. Simon Lagies, Lukas M. Braun, and Manuel Schlimpert wrote the manuscript.

Compliance with ethical standards

Informed consent Informed consent was obtained for KHM1106 cell line usage and approved by the local Ethics Committee Freiburg (126/17 and 371/14) and registered at the German Clinical Trials Register (DRKS-ID DRKS00007561).

Conflict of interest The authors declare that they have no conflict of interest.

References

1. Rahib L, Smith BD, Aizenberg R, Rosenzweig AB, Fleshman JM, Matrisian LM. Projecting cancer incidence and deaths to 2030: the unexpected burden of thyroid, liver, and pancreas cancers in the United States. Cancer Res. 2014;74:2913–21. https://doi.org/10.1158/0008-5472.CAN-14-0155.

2. Siegel R, Ma J, Zou Z, Jemal A. Cancer statistics, 2014. CA Cancer J Clin. 2014;64:9–29. https://doi.org/10.3322/caac.21208.
3. Siegel R, Naishadham D, Jemal A. Cancer statistics, 2013. CA Cancer J Clin. 2013;63:11–30. https://doi.org/10.3322/caac.21166.
4. Neoptolemos JP, Kleeff J, Michl P, Costello E, Greenhalf W, Palmer DH. Therapeutic developments in pancreatic cancer: current and future perspectives. Nat Rev Gastroenterol Hepatol. 2018;15:333–48. https://doi.org/10.1038/s41575-018-0005-x.
5. Kleeff J, Korc M, Apte M, La Vecchia C, Johnson CD, Biankin AV, et al. Pancreatic cancer. Nat Rev Dis Primers. 2016;2:16022. https://doi.org/10.1038/nrdp.2016.22.
6. Partensky C. Toward a better understanding of pancreatic ductal adenocarcinoma: glimmers of hope? Pancreas. 2013;42:729–39. https://doi.org/10.1097/MPA.0b013e318288107a.
7. Schnelldorfer T, Ware AL, Sarr MG, Smyrk TC, Zhang L, Qin R, et al. Long-term survival after pancreatoduodenectomy for pancreatic adenocarcinoma: is cure possible? Ann Surg. 2008;247:456–62. https://doi.org/10.1097/SLA.0b013e3181613142.
8. Oettle H, Neuhaus P, Hochhaus A, Hartmann JT, Gellert K, Ridwelski K, et al. Adjuvant chemotherapy with gemcitabine and long-term outcomes among patients with resected pancreatic cancer: the CONKO-001 randomized trial. JAMA. 2013;310:1473–81. https://doi.org/10.1001/jama.2013.279201.
9. Gillen S, Schuster T, Zum Meyer Büschenfelde C, Friess H, Kleeff J. Preoperative/neoadjuvant therapy in pancreatic cancer: a systematic review and meta-analysis of response and resection percentages. PLoS Med. 2010;7:e1000267. https://doi.org/10.1371/journal.pmed.1000267.
10. Scarà S, Bottoni P, Scatena R. CA 19-9: biochemical and clinical aspects. Adv Exp Med Biol. 2015;867:247–60. https://doi.org/10.1007/978-94-017-7215-0_15.
11. Takai E, Yachida S. Circulating tumor DNA as a liquid biopsy target for detection of pancreatic cancer. World J Gastroenterol. 2016;22:8480–8. https://doi.org/10.3748/wjg.v22.i38.8480.
12. Cote GA, Gore AJ, McElyea SD, Heathers LE, Xu H, Sherman S, et al. A pilot study to develop a diagnostic test for pancreatic ductal adenocarcinoma based on differential expression of select miRNA in plasma and bile. Am J Gastroenterol. 2014;109:1942–52. https://doi.org/10.1038/ajg.2014.331.
13. Nagayoshi Y, Nakamura M, Matsuoka K, Ohtsuka T, Mori Y, Kono H, et al. Profiling of autoantibodies in sera of pancreatic cancer patients. Ann Surg Oncol. 2014;21(Suppl 3):S459–65. https://doi.org/10.1245/s10434-014-3574-0.
14. Pan S, Chen R, Crispin DA, May D, Stevens T, McIntosh MW, et al. Protein alterations associated with pancreatic cancer and chronic pancreatitis found in human plasma using global quantitative proteomics profiling. J Proteome Res. 2011;10:2359–76. https://doi.org/10.1021/pr101148r.
15. Melo SA, Luecke LB, Kahlert C, Fernandez AF, Gammon ST, Kaye J, et al. Glypican-1 identifies cancer exosomes and detects early pancreatic cancer. Nature. 2015;523:177–82. https://doi.org/10.1038/nature14581.
16. Ritchie SA, Akita H, Takemasa I, Eguchi H, Pastural E, Nagano H, et al. Metabolic system alterations in pancreatic cancer patient serum: potential for early detection. BMC Cancer. 2013;13:416. https://doi.org/10.1186/1471-2407-13-416.
17. Mayerle J, Kalthoff H, Reszka R, Kamlage B, Peter E, Schniewind B, et al. Metabolic biomarker signature to differentiate pancreatic ductal adenocarcinoma from chronic pancreatitis. Gut. 2018;67:128–37. https://doi.org/10.1136/gutjnl-2016-312432.
18. Di Gangi IM, Mazza T, Fontana A, Copetti M, Fusilli C, Ippolito A, et al. Metabolomic profile in pancreatic cancer patients: a consensus-based approach to identify highly discriminating metabolites. Oncotarget. 2016;7:5815–29. https://doi.org/10.18632/oncotarget.6808.
19. Mehta KY, Wu H-J, Menon SS, Fallah Y, Zhong X, Rizk N, et al. Metabolomic biomarkers of pancreatic cancer: a meta-analysis study. Oncotarget. 2017;8:68899–915. https://doi.org/10.18632/oncotarget.20324.
20. Kobayashi T, Nishiumi S, Ikeda A, Yoshie T, Sakai A, Matsubara A, et al. A novel serum metabolomics-based diagnostic approach to pancreatic cancer. Cancer Epidemiol Biomark Prev. 2013;22:571–9. https://doi.org/10.1158/1055-9965.EPI-12-1033.
21. Borek E, Baliga BS, Gehrke CW, Kuo CW, Belman S, Troll W, et al. High turnover rate of transfer RNA in tumor tissue. Cancer Res. 1977;37:3362–6.
22. Tusup M, Kundig T, Pascolo S. Epitranscriptomics of cancer. World J Clin Oncol. 2018;9:42–55. https://doi.org/10.5306/wjco.v9.i3.42.
23. Kammerer B, Frickenschmidt A, Muller CE, Laufer S, Gleiter CH, Liebich H. Mass spectrometric identification of modified urinary nucleosides used as potential biomedical markers by LC-ITMS coupling. Anal Bioanal Chem. 2005;382:1017–26. https://doi.org/10.1007/s00216-005-3232-2.
24. Zhang Y-R, Shi L, Wu H, Tang D-D, Wang S-M, Liu H-M, et al. Urinary modified nucleosides as novel biomarkers for diagnosis and prognostic monitoring of urothelial bladder cancer. Tumori. 2014;100:660–6. https://doi.org/10.1700/1778.19274.
25. Willmann L, Erbes T, Halbach S, Brummer T, Jäger M, Hirschfeld M, et al. Exometabolom analysis of breast cancer cell lines: metabolic signature. Sci Rep. 2015;5:13374. https://doi.org/10.1038/srep13374.
26. Hsu W-Y, Chen WT-L, Lin W-D, Tsai F-J, Tsai Y, Lin C-T, et al. Analysis of urinary nucleosides as potential tumor markers in human colorectal cancer by high performance liquid chromatography/electrospray ionization tandem mass spectrometry. Clin Chim Acta. 2009;402:31–7. https://doi.org/10.1016/j.cca.2008.12.009.
27. Frickenschmidt A, Frohlich H, Bullinger D, Zell A, Laufer S, Gleiter CH, et al. Metabonomics in cancer diagnosis: mass spectrometry-based profiling of urinary nucleosides from breast cancer patients. Biomarkers. 2008;13:435–49. https://doi.org/10.1080/13547500802012858.
28. Lu Z, Wang Q, Wang M, Fu S, Zhang Q, Zhang Z, et al. Using UHPLC Q-rap/MS as a complementary technique to in-depth mine UPLC Q-TOF/MS data for identifying modified nucleosides in urine. J Chromatogr B Analyt Technol Biomed Life Sci. 2017;1051:108–17. https://doi.org/10.1016/j.jchromb.2017.03.002.
29. Pringle SD, Giles K, Wildgoose JL, Williams JP, Slade SE, Thalassinos K, et al. An investigation of the mobility separation of some peptide and protein ions using a new hybrid quadrupole/travelling wave IMS/oa-ToF instrument. Int J Mass Spectrom. 2007;261:1–12. https://doi.org/10.1016/j.ijms.2006.07.021.
30. Stephan S, Jakob C, Hippler J, Schmitz OJ. A novel four-dimensional analytical approach for analysis of complex samples. Anal Bioanal Chem. 2016;408:3751–9. https://doi.org/10.1007/s00216-016-9460-9.
31. Stark TD, Ranner J, Stiglbauer B, Weiss P, Stark S, Balemba OB, et al. Construction and application of a database for a five dimensional identification of natural compounds in Garcinia species by means of UPLC-ESI-TWIMS-TOF-MS-introducing gas phase polyphenol conformer drift time distribution intensity ratios. J Agric Food Chem. 2018. https://doi.org/10.1021/acs.jafc.8b06157 .
32. Rister AL, Martin TL, Dodds ED. Application of group I metal adduction to the separation of steroids by traveling wave ion mobility spectrometry. J Am Soc Mass Spectrom. 2019;30:248–55. https://doi.org/10.1007/s13361-018-2085-9.
33. Keelor JD, Zambrzycki S, Li A, Clowers BH, Fernandez FM. Atmospheric pressure drift tube ion mobility-Orbitrap mass spectrometry: initial performance characterization. Anal Chem. 2017;89:11301–9. https://doi.org/10.1021/acs.analchem.7b01866.

34. Jeanne Dit Fouque K, Bisram V, Hegemann JD, Zirah S, Rebuffat S, Fernandez-Lima F. Structural signatures of the class III lasso peptide BI-32169 and the branched-cyclic topoisomers using trapped ion mobility spectrometry–mass spectrometry and tandem mass spectrometry. Anal Bioanal Chem. 2019. https://doi.org/10.1007/s00216-019-01613-8.
35. Kanu AB, Hampikian G, Brandt SD, Hill HH Jr. Ribonucleotide and ribonucleoside determination by ambient pressure ion mobility spectrometry. Anal Chim Acta. 2010;658:91–7. https://doi.org/10.1016/j.aca.2009.10.058.
36. Quinn R, Basanta-Sanchez M, Rose RE, Fabris D. Direct infusion analysis of nucleotide mixtures of very similar or identical elemental composition. J Mass Spectrom. 2013;48:703–12. https://doi.org/10.1002/jms.3207.
37. Rose RE, Quinn R, Sayre JL, Fabris D. Profiling ribonucleotide modifications at full-transcriptome level: a step toward MS-based epitranscriptomics. RNA. 2015;21:1361–74. https://doi.org/10.1261/rna.049429.114.
38. Loukopoulos P, Kanetaka K, Takamura M, Shibata T, Sakamoto M, Hirohashi S. Orthotopic transplantation models of pancreatic adenocarcinoma derived from cell lines and primary tumors and displaying varying metastatic activity. Pancreas. 2004;29:193–203.
39. Berrozpe G, Schaeffer J, Peinado MA, Real FX, Perucho M. Comparative analysis of mutations in the p53 and K-ras genes in pancreatic cancer. Int J Cancer. 1994;58:185–91.
40. Kyriazis AA, Kyriazis AP, Sternberg CN, Sloane NH, Loveless JD. Morphological, biological, biochemical, and karyotypic characteristics of human pancreatic ductal adenocarcinoma Capan-2 in tissue culture and the nude mouse. Cancer Res. 1986;46:5810–5.
41. Fahrmann JF, Bantis LE, Capello M, Scelo G, Dennison JB, Patel N, et al. A plasma-derived protein-metabolite multiplexed panel for early-stage pancreatic cancer. J Natl Cancer Inst. 2018. https://doi.org/10.1093/jnci/djy126.
42. Metzgar RS, Gaillard MT, Levine SJ, Tuck FL, Bossen EH, Borowitz MJ. Antigens of human pancreatic adenocarcinoma cells defined by murine monoclonal antibodies. Cancer Res. 1982;42:601–8.
43. Moore PS, Sipos B, Orlandini S, Sorio C, Real FX, Lemoine NR, et al. Genetic profile of 22 pancreatic carcinoma cell lines. Analysis of K-ras, p53, p16 and DPC4/Smad4. Virchows Arch. 2001;439:798–802.
44. Yunis AA, Arimura GK, Russin DJ. Human pancreatic carcinoma (MIA PaCa-2) in continuous culture: sensitivity to asparaginase. Int J Cancer. 1977;19:128–35.
45. Sun C, Yamato T, Furukawa T, Ohnishi Y, Kijima H, Horii A. Characterization of the mutations of the K-ras, p53, p16, and SMAD4 genes in 15 human pancreatic cancer cell lines. Oncol Rep. 2001;8:89–92.
46. Lieber M, Mazzetta J, Nelson-Rees W, Kaplan M, Todaro G. Establishment of a continuous tumor-cell line (panc-1) from a human carcinoma of the exocrine pancreas. Int J Cancer. 1975;15:741–7.
47. Dodds JN, May JC, McLean JA. Correlating resolving power, resolution and collision cross section: unifying cross platform assessment of separation efficiency in ion mobility spectrometry. Anal Chem. 2017;89:12176–84. https://doi.org/10.1021/acs.analchem.7b02827.
48. Smith DP, Knapman TW, Campuzano I, Malham RW, Berryman JT, Radford SE, et al. Deciphering drift time measurements from travelling wave ion mobility spectrometry-mass spectrometry studies. Eur J Mass Spectrom (Chichester). 2009;15:113–30. https://doi.org/10.1255/ejms.947.
49. Chong J, Soufan O, Li C, Caraus I, Li S, Bourque G, et al. MetaboAnalyst 4.0: towards more transparent and integrative metabolomics analysis. Nucleic Acids Res. 2018;46:W486–94. https://doi.org/10.1093/nar/gky310.
50. Cantara WA, Crain PF, Rozenski J, McCloskey JA, Harris KA, Zhang X, et al. The RNA modification database, RNAMDB: 2011 update. Nucleic Acids Res. 2011;39:D195–201. https://doi.org/10.1093/nar/gkq1028.
51. Willmann L, Erbes T, Krieger S, Trafkowski J, Rodamer M, Kammerer B. Metabolome analysis via comprehensive two-dimensional liquid chromatography: identification of modified nucleosides from RNA metabolism. Anal Bioanal Chem. 2015;407:3555–66. https://doi.org/10.1007/s00216-015-8516-6.
52. Li H-Y, Wang S-M, Liu H-M, Li J, Han D, Bu S-S, et al. Analysis of modified nucleosides in the urine of patients with malignant cancer by liquid chromatography/electrospray ionization mass spectrometry. Rapid Commun Mass Spectrom. 2008;22:3161–71. https://doi.org/10.1002/rcm.3721.
53. Schlimpert M, Lagies S, Budnyk V, Müller B, Walz G, Kammerer B. Metabolic phenotyping of Anks3 depletion in mIMCD-3 cells - a putative nephronophthisis candidate. Sci Rep. 2018;8:9022. https://doi.org/10.1038/s41598-018-27389-y.
54. Paglia G, Williams JP, Menikarachchi L, Thompson JW, Tyldesley-Worster R, Halldórsson S, et al. Ion mobility derived collision cross sections to support metabolomics applications. Anal Chem. 2014;86:3985–93. https://doi.org/10.1021/ac500405x.